

EurJIC

European Journal of Inorganic Chemistry

 **Chemistry
Europe**
European Chemical
Societies Publishing

Accepted Article

Title: Copper(II)-Doped ZIF-8 as a Reusable and Size Selective Heterogeneous Catalyst for the Hydrogenation of Alkenes using Hydrazine Hydrate

Authors: Nagarathinam Nagarjun, Kannan Arthy, and Amarajothi Dhakshinamoorthy

This manuscript has been accepted after peer review and appears as an Accepted Article online prior to editing, proofing, and formal publication of the final Version of Record (VoR). This work is currently citable by using the Digital Object Identifier (DOI) given below. The VoR will be published online in Early View as soon as possible and may be different to this Accepted Article as a result of editing. Readers should obtain the VoR from the journal website shown below when it is published to ensure accuracy of information. The authors are responsible for the content of this Accepted Article.

To be cited as: *Eur. J. Inorg. Chem.* 10.1002/ejic.202100126

Link to VoR: <https://doi.org/10.1002/ejic.202100126>

WILEY-VCH

Copper(II)-Doped ZIF-8 as a Reusable and Size Selective Heterogeneous Catalyst for the Hydrogenation of Alkenes using Hydrazine Hydrate

Mr. Nagarathinam Nagarjun, Ms. Kannan Arthy, Prof. Amarajothi Dhakshinamoorthy*

School of Chemistry, Madurai Kamaraj University, Madurai 625021, Tamil Nadu, India.

E-mail: admguru@gmail.com; adm.chem@mkuniversity.org; M:+91 99764 73669

<https://mkuniversity.ac.in/new/school/sc/dhakshinamoorthy.php>

Twitter: Madurai Kamaraj University @mku_official

Abstract

In recent years, synthesis of mixed-metal organic frameworks has received considerable attention due to their superior performance than metal organic frameworks (MOFs) with mono-metallic MOFs. In the present manuscript, Cu^{2+} ions are doped within the framework of ZIF-8 to obtain Cu@ZIF-8 and is characterized by powder X-ray diffraction (XRD), Fourier transform infrared (FT-IR), UV-Visible diffuse reflectance spectra (DRS), scanning electron microscope (SEM) and transmission electron microscope (TEM) studies. The reaction conditions are optimized with styrene as a substrate using Cu@ZIF-8 as solid catalyst. Heterogeneity of the reaction is confirmed by leaching test and the solid is reusable for three cycles with no diminishing activity. Further, the structural integrity is also retained after hydrogenation of styrene. The size selective catalysis of Cu@ZIF-8 is demonstrated by comparing the activity of Cu^{2+} ions adsorbed over ZIF-8 solid (Cu/ZIF-8) in the hydrogenation of 1-hexene, 1-octene, cyclohexene, cyclooctene and t-stilbene. The catalytic results indicate that Cu/ZIF-8 shows superior activity than Cu@ZIF-8 for all these olefins due to the lack of diffusion to access the active sites (Cu^{2+}). In contrast, Cu@ZIF-8 exhibits higher activity for those olefins with lower molecular dimensions (1-hexene, 1-octene) than the pores of ZIF-8 to facilitate facile diffusion inside the pores ZIF-8 while poor activity is observed with t-stilbene due to its larger molecular dimension than the pore apertures of ZIF-8. These catalytic data clearly establish the size selective hydrogenation of Cu@ZIF-8 due to the effective confinement provided by ZIF-8 framework and the presence of the active sites within the framework. Furthermore, this is the first report showing the size selective hydrogenation of olefins promoted by Cu@ZIF-8 (mixed-metal MOFs) compared to other noble metal nanoparticles (NPs) embedded over MOFs as catalysts.

1. Introduction

MOFs are crystalline porous solids whose structure is composed between metal ions or clusters with rigid organic linkers leading to the formation of one, two and three dimensional solids.^[1-4] One of the unique properties of MOFs compared to other analogous porous crystalline solids is their high surface area and pore volume.^[5-7] Another interesting feature of MOFs than to analogous solids is their tunable pore volume or surface area.^[8] Furthermore, surface area and pore size of a MOF can also be predicted through the appropriate selection of organic linkers and metal ions.^[9] Due to the presence of well defined pores in the architecture of MOFs, they can be readily employed as a suitable host for the encapsulation of guests like metal nanoparticles (NPs), metal oxide NPs and metal complexes and their activity was tested in many fields including catalysis,^[10-12] photocatalysis^[13] and photodegradation of pollutants.^[14]

Selective hydrogenation of olefins to their respective saturated hydrocarbons is an important industrial process and it is frequently performed for the production of fine chemicals, petrochemistry and drug intermediates.^[15, 16] Very often, noble metal NPs like Pd, Pt, Au and Ru supported on porous solids have been reported as heterogeneous catalysts for hydrogenation reactions.^[17] The main purpose of loading these metal NPs on a solid support is to prevent their growth of particle size by agglomeration and thereby harvesting their catalytic performance in a confined space. In this aspect, zeolites were one of the extensively employed porous solids to achieve size selective catalysis in broad ranges of organic reactions due to the effective stabilization of metal NPs in their well defined channels and pores.^[18-21] Inspired by these research findings, many research groups have focused on the encapsulation of metal NPs over MOFs and their activities are examined in the size selective catalysis.^[22, 23]

One of the prerequisites of MOFs to behave as hosts for metal NPs is their stability during the loading of metal NPs. In this aspect, metal NPs encapsulated over MOFs have been reported as heterogeneous catalysts for the size selective hydrogenation of olefins using Pd nanocubes@ZIF-8 under photocatalytic conditions,^[24] Pd@ZIF-8,^[25, 26] Pt@ZIF-8,^[27] Pt@ZIF-8 with different particle size,^[28] Pt/UIO-66,^[29] SIM-1@Pt/Al₂O₃ (SIM: Substituted Imidazolate),^[30] Pt-Cu frame@HKUST-1^[31] and RhCoNi@ZIF-67(Co)/RhCoNi@MOF-74(Ni).^[32] On the other hand, very recently, various kinds of Cu-based heterogeneous catalysts were reported as heterogeneous solid catalysts for hydrogenation reaction.^[33, 34]

ZIF-8 (ZIF: Zeolitic Imidazolate Frameworks) is constituted from tetrahedral units, in which Zn^{2+} ions are coordinated to four imidazolate ligands resulting in the formation of a three dimensional frameworks with sodalite topology $[\text{Zn}(\text{Melm})_2]$ (Melm: 2-methylimidazole).^[35, 36] The structural analysis of ZIF-8 reveals the existence of sodalite cages with a pore diameter of 11.6 Å and the opening between two cages is 3.4 Å. ZIF-based solids were employed for large numbers of applications including gas storage,^[37, 38] catalysis,^[4, 39] sensing,^[40] chemical separation^[41] and drug delivery.^[42] Some of the notable features that make ZIFs as appropriate solids for these applications include high surface area, high density of functional groups, pH responsive degradation, high loading of drug, high thermal and chemical stabilities.^[43, 44] ZIFs and their composites have also been reported as multifunctional solids with superior performances.^[45, 46]

In recent years, preparation of mixed metal MOFs has received considerable attentions mainly due to their superior catalytic activities than the MOF containing single metal ions.^[47, 48] The enhanced activity may be due to the combinations of both metal ions or it can be due to a single metal ion with uniform distribution while other metal ion stabilizes the MOF framework. Further, Schneider and co-workers have reported the synthesis of Cu^{2+} -doped ZIF-8 (Cu@ZIF-8) and its catalytic activity was tested in the cycloaddition and condensation reactions.^[49] Although considerable progress made in using ZIF-8 as scaffolds for the loading of metal NPs in size selective hydrogenation, no attempts were made to use mixed-metal MOFs as heterogeneous catalysts involving the framework cations as active sites to promote hydrogenation of olefins. Further, the facile doping of Cu^{2+} ions within the framework of ZIF-8 to obtain mixed metal ZIF-8 solids prompted us to report the use of Cu@ZIF-8 as size selective heterogeneous solid catalyst in the hydrogenation of olefins with different dimensions using hydrazine hydrate as reducing agent at room temperature. Furthermore, a control catalyst was also prepared by adsorbing Cu^{2+} over ZIF-8 ($\text{Cu}^{2+}/\text{ZIF-8}$) to prove the size selective hydrogenation of Cu@ZIF-8 . Furthermore, this work nicely illustrates that the rate of hydrogenation of olefins is enhanced with Cu@ZIF-8 compared to ZIF-8 under similar conditions. Besides, catalyst stability is also proved by performing leaching and reusability experiments. In addition, Cu@ZIF-8 exhibits wide substrate scope in the hydrogenation of substituted styrenes under the optimized reaction conditions.

2. Results and Discussions

Cu@ZIF-8 solid was synthesized by adopting previously reported procedure.^[49] The catalytic performance of Cu@ZIF-8 was studied in the hydrogenation of olefins and its activity is compared with Cu/ZIF-8 under similar experimental conditions to demonstrate the size selective catalysis of Cu@ZIF-8. The visual color changes from ZIF-8 to Cu@ZIF-8 and Cu/ZIF-8 upon doping and adsorbing of Cu^{2+} ions, respectively. (Chart S1, Supporting Information). These images clearly suggest the presence of Cu^{2+} ions at different chemical environments in these two solids. Further, Cu@ZIF-8 was characterized by powder XRD, FT-IR, UV-Visible DRS, SEM methods and the observed results are in line with the reported results.^[49, 50] Briefly, powder XRD patterns of ZIF-8, Cu@ZIF-8 and Cu/ZIF-8 are shown in Figure 1 and they clearly indicate that the structural integrity and crystallinity are not altered upon doping/adsorbing with Cu^{2+} ions. The facile doping of Cu^{2+} ions without affecting crystallinity of ZIF-8 is mainly due to the closer ionic radii between Cu^{2+} (0.71 Å) and Zn^{2+} (0.74 Å) ions. In contrast, Li and co-workers have reported the introduction of Ni^{2+} in ZIF-8 framework by mechanochemical method and observing additional peaks in the powder XRD pattern due to the formation of clusters between Ni^{2+} ion and 2-methylimidazole that are confined in ZIF-8 cavities.^[51, 52] Interestingly, the doping of Cu^{2+} ions over ZIF-8 did not show any extra peaks other than ZIF-8, thus confirming the existence of Cu^{2+} ions exclusively within the framework of ZIF-8.

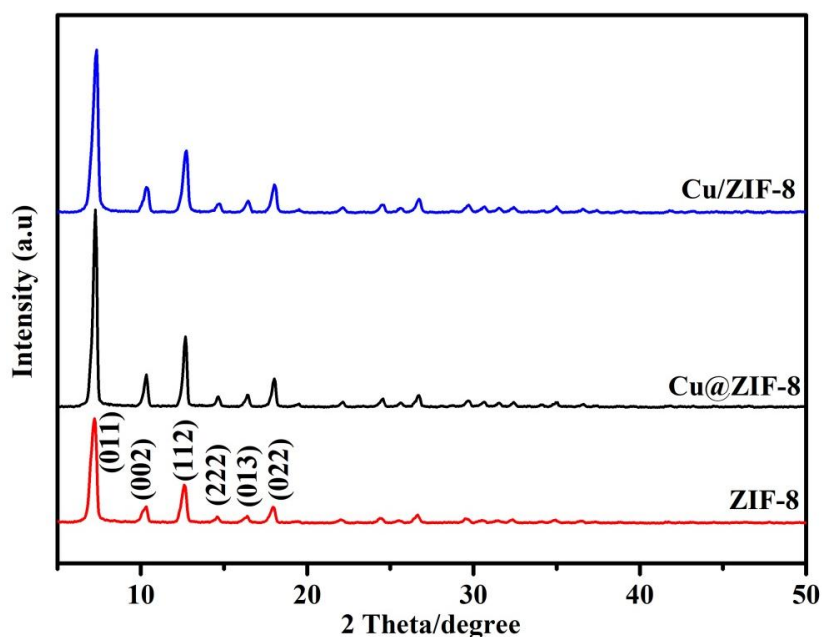


Figure 1. Powder XRD patterns of (a) ZIF-8, (b) Cu@ZIF-8 and (c) Cu/ZIF-8.

Figure 2 shows FT-IR spectra of ZIF-8, Cu@ZIF-8 and Cu/ZIF-8 solids. A sharp peak at 423 cm^{-1} corresponds to the stretching vibration of Zn-N bond indicating the coordination of Zn^{2+} ions to nitrogen atoms from 2-methylimidazole linker.^[53] Further, the stretching vibrations from 1100 to 1300 cm^{-1} are assigned to C-H vibrations, while the peak located at 1466 cm^{-1} is assigned to C=N stretching vibration. In addition, the peak at 1229 cm^{-1} confirms the trembling of C-N bond in the imidazole ring. A characteristic stretching frequency of Cu-N bond in Cu@ZIF-8 solid is located around 575 cm^{-1} which is in good correlation with earlier report.^[54] However, this band is not seen in ZIF-8 and Cu/ZIF-8, thus suggesting the facile doping of Cu^{2+} ion within the framework of ZIF-8 to afford Cu@ZIF-8.

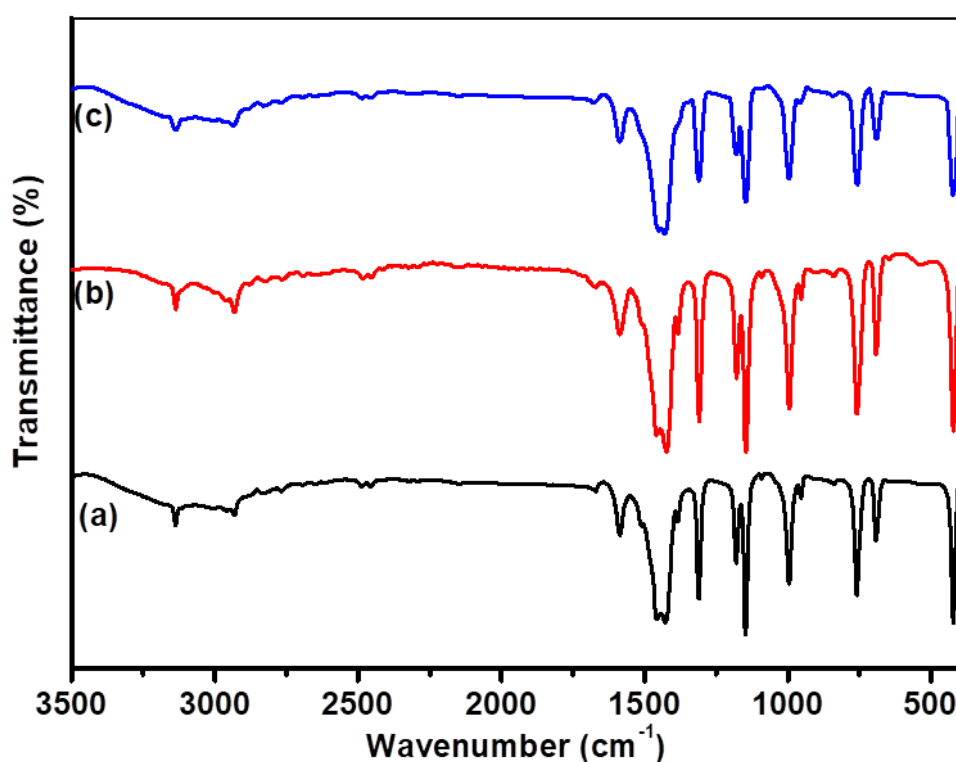


Figure 2. FT-IR spectra of (a) ZIF-8, (b) Cu@ZIF-8 and (c) Cu/ZIF-8 solids.

Similarly, the presence of Cu^{2+} ion in the ZIF-8 framework was further confirmed by measuring UV-Vis DRS for ZIF-8, Cu@ZIF-8 and Cu/ZIF-8. The observed results are shown in Figure 3. The doping of Cu^{2+} ion shifts the absorption edge of ZIF-8 solid from UV to visible region. Furthermore, Cu@ZIF-8 displayed well-defined two bands, one at 490 nm while the second broad band starting at 600 nm , which is due to the d-d transition of Cu^{2+} ion. These results convincingly demonstrate the presence of Cu^{2+} ion in

Cu@ZIF-8 solid. Further, Cu/ZIF-8 also shows similar bands compared to Cu@ZIF-8. In contrast, ZIF-8 showed no such bands due to the absence of Cu^{2+} ions.

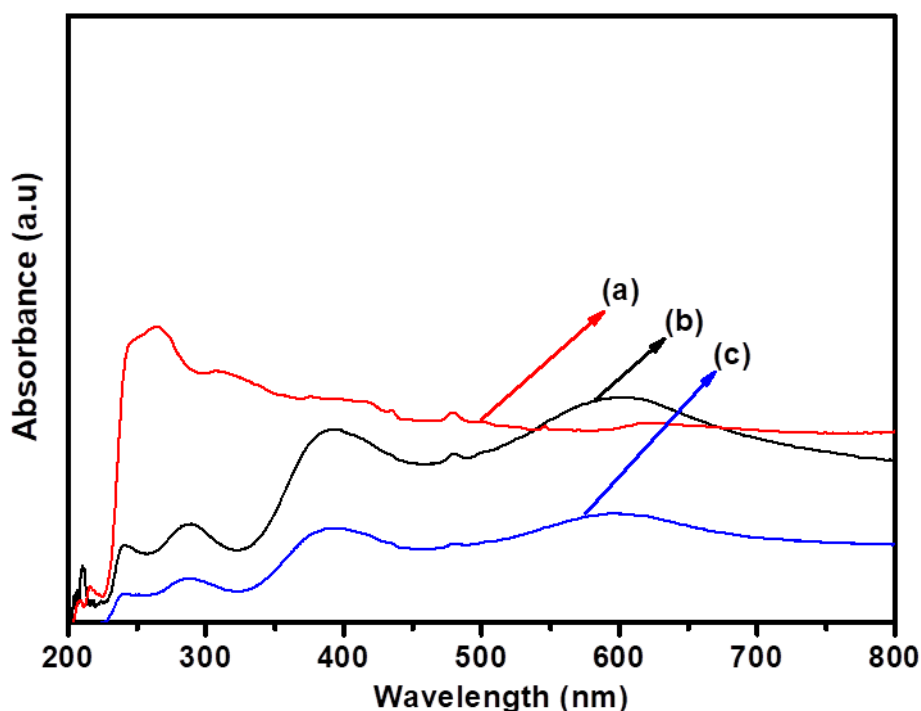


Figure 3. UV-Vis DRS spectra of (a) ZIF-8, (b) Cu@ZIF-8 and (c) Cu/ZIF-8 solids.

After out-gassing the samples under vacuum at 150 °C for 10 h, permanent porosities of ZIF-8, Cu@ZIF-8 and Cu/ZIF-8 materials were measured by nitrogen adsorption-desorption studies at 77 K (Figures S23-S25). The observed data exhibit type I isotherms which are in agreement with earlier report.^[49] The BET surface area of Cu@ZIF-8 and Cu/ZIF-8 solids was 1590 and 1612 m²/g which are slightly lower than ZIF-8 (1712 m²/g). The pore volume of ZIF-8, Cu@ZIF-8 and Cu/ZIF-8 was 0.571, 0.518 and 0.517 cm³/g, respectively. The pore size of ZIF-8, Cu@ZIF-8 and Cu/ZIF-8 was 1.29, 1.21 and 1.20 nm, respectively. These results are in agreement with recent results.^[49]

On the other hand, the morphology of ZIF-8 and Cu@ZIF-8 was measured by SEM images and the observed results are presented in Figure 4. ZIF-8 solid exhibited well-defined truncated rhombic dodecahedron morphology and it is not altered upon doping with Cu^{2+} ions within the framework of ZIF-8. These characterization data are in agreement that Zn^{2+} and Cu^{2+} ions are part of the framework leading to the formation of a crystalline solid with uniform morphology. In addition, it was reported by us that

Cu@ZIF-8 showed a characteristic EPR signal and is due to the presence of Cu^{2+} ion while such band is absent in ZIF-8.^[49] Furthermore, elemental composition of Cu@ZIF-8 was measured by EDX analysis and the weight percentage of copper is 2.46%. Also, the elemental mapping of Cu@ZIF-8 was shown in Figure 5 and clearly indicating the existence of copper throughout the framework. Hence, the doping of Cu^{2+} ions within the framework of ZIF-8 is indirectly confirmed by these results.

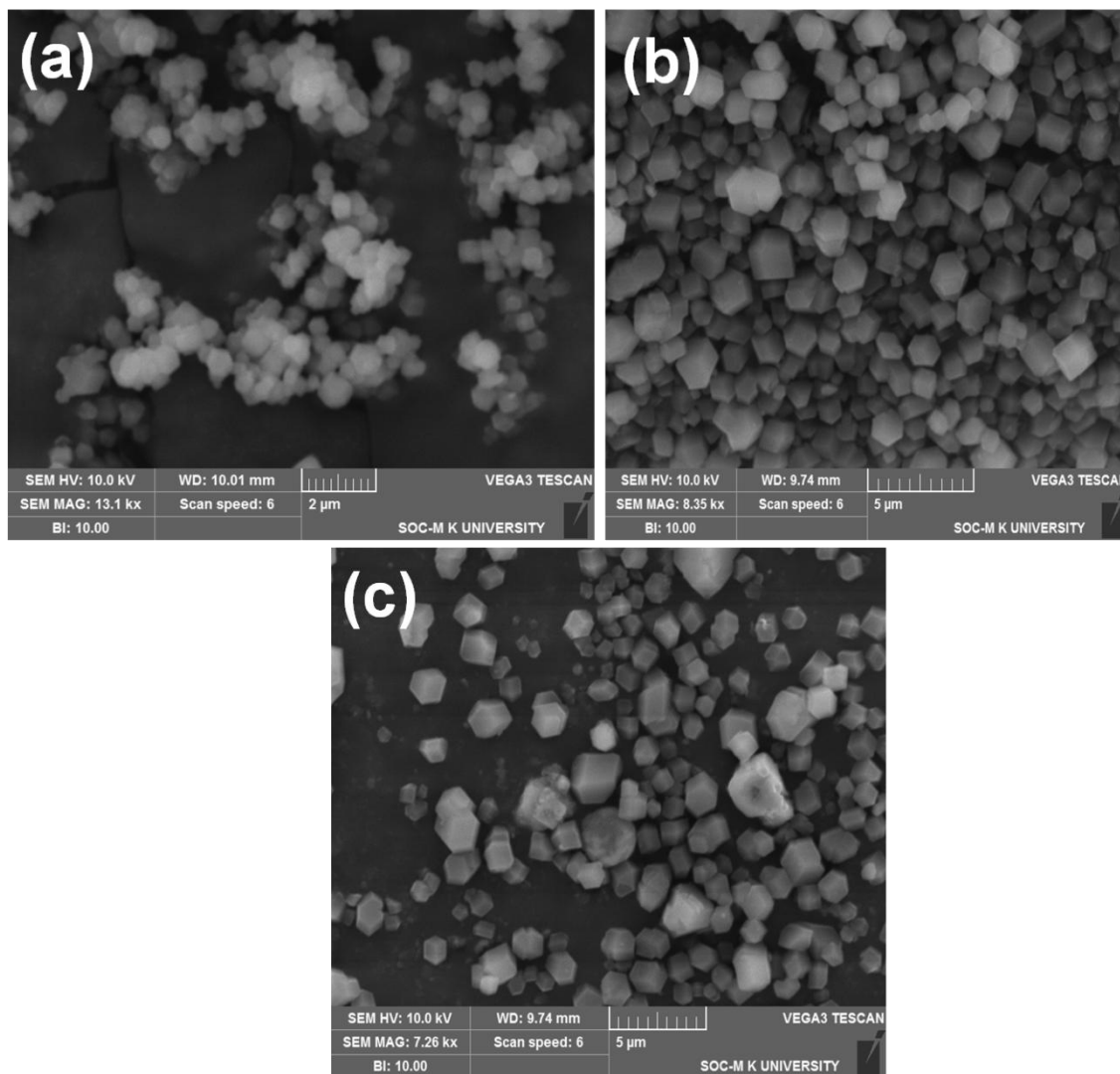


Figure 4. SEM images of (a) ZIF-8, (b) Cu@ZIF-8 and (c) after 3rd reuse of Cu@ZIF-8.

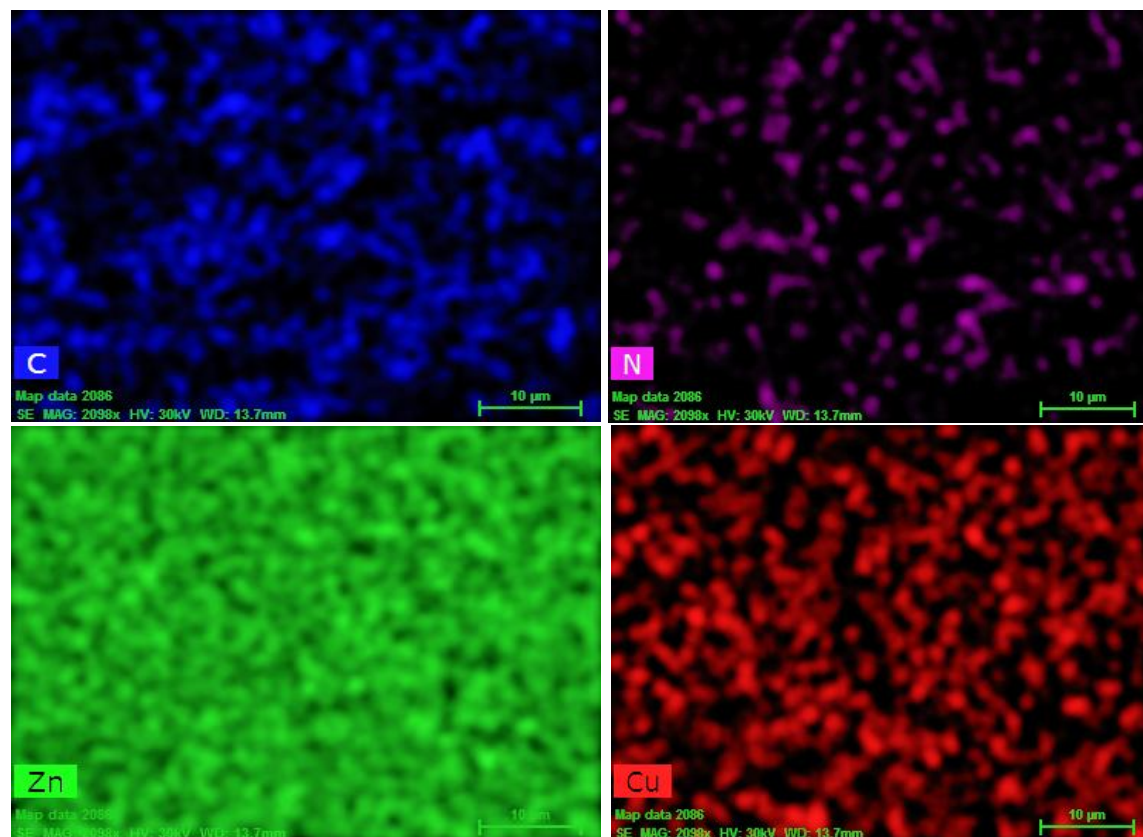


Figure 5. SEM-EDX analysis of Cu@ZIF-8.

TEM images were measured for Cu@-ZIF-8 and Cu/ZIF-8 to compare the morphology and the location of Cu^{2+} ions in these solids (Figure 6). These images clearly indicate that both samples exhibit as a well-defined truncated rhombic dodecahedron structure which is the ideal morphology reported for ZIF-8. These results unambiguously prove that the surface morphology and the framework structure of ZIF-8 are not altered during the doping of Cu^{2+} ions and are in line with SEM results.^[49] In contrast, TEM images of Cu/ZIF-8 illustrate that the Cu^{2+} ions are adsorbed on the outer surface of the crystals while such adsorption is not seen with Cu@ZIF-8, indicating the facile doping of Cu^{2+} ions. Further, the characteristic lattice spacing of 0.284 nm was observed for Cu^{2+} ions adsorbed on (011) plane of ZIF-8 phase.^[55, 56]

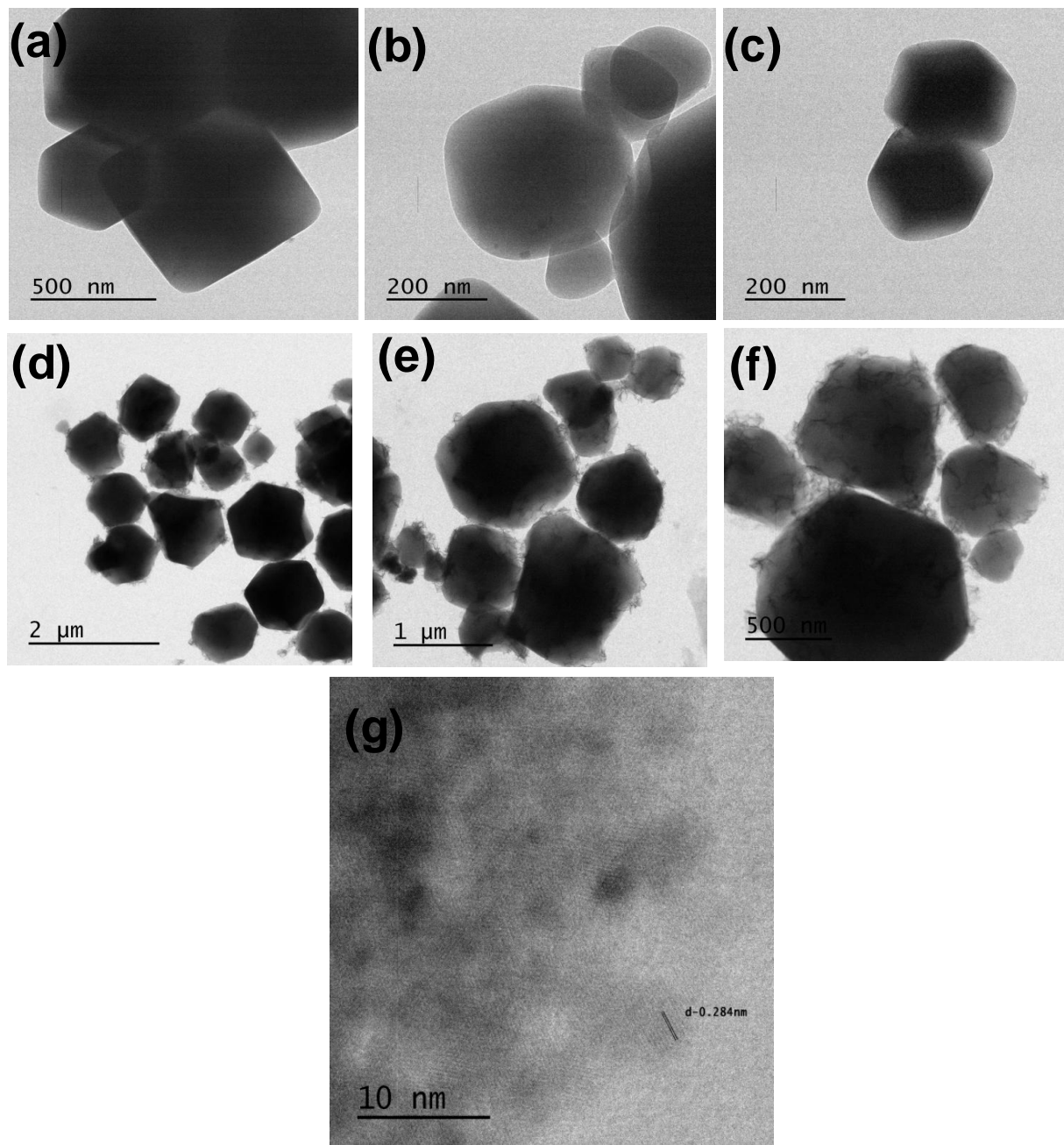


Figure 6. TEM images of (a), (b), (c) of Cu@ZIF-8 and (d), (e), (f) of Cu/ZIF-8. The d-spacing of Cu²⁺ ions is shown in (g).

As commented earlier, size selective hydrogenations have been reported with noble metal NPs encapsulated over MOFs like ZIF-8.^[23] Hence, one of the main objectives of this work is to demonstrate the catalytic activity of Cu²⁺ ions in the size selective hydrogenation of olefins under mild reaction

conditions without the requirement of noble metal NPs. Interestingly, the framework Cu^{2+} ions promote the hydrogenation of olefins while ZIF-8 framework offers a confined environment to achieve size selective catalysis. In order to prove this hypothesis, the reaction conditions were optimized in terms of catalyst loading, $\text{N}_2\text{H}_4\cdot\text{H}_2\text{O}$ concentration by selecting styrene as a model substrate using Cu@ZIF-8 as a solid catalyst. The observed catalytic data are presented in Table 1. A blank control experiment in the absence of catalyst showed 20% conversion of styrene with $\text{N}_2\text{H}_4\cdot\text{H}_2\text{O}$ as reducing agent in ethanol at room temperature after 14 h. On the other hand, ZIF-8 exhibited 36% conversion of styrene in ethanol under identical conditions. Interestingly, Cu@ZIF-8 afforded quantitative conversion of styrene in ethanol under similar experimental conditions. These catalytic results clearly prove the efficient performance of Cu^{2+} ions in achieving complete conversion of styrene. Figure 7 shows the time conversion plot for the transformation of styrene to ethylbenzene using Cu@ZIF-8 as solid catalyst. Although the conversion of styrene was 80% in methanol while other solvents showed poor to moderate conversions using Cu@ZIF-8 as catalyst under same conditions. Further, the conversion of styrene reached to 51% under neat conditions after 14 h at room temperature. The conversion of styrene was unsuccessful with isopropanol as a reducing agent under same conditions.

In another set of experiments, the conversion of styrene was significantly reduced upon lowering the catalyst loadings and Figure 8 indicates their respective time conversion plots. Similarly, the influence of $\text{N}_2\text{H}_4\cdot\text{H}_2\text{O}$ concentration in the conversion of styrene was monitored and achieving the highest conversion with the maximum dosage of $\text{N}_2\text{H}_4\cdot\text{H}_2\text{O}$ under identical conditions (Figure 9). A control experiment with pyridine as a catalyst poison was performed in the hydrogenation of styrene using Cu@ZIF-8 in ethanol at room temperature for 14 h. Surprisingly, the conversion of styrene was completely quenched in the presence of pyridine thus suggesting the strong coordination of pyridine with $\text{Zn}^{2+}/\text{Cu}^{2+}$ ions. As a consequence, the interaction of these metal ions with $\text{N}_2\text{H}_4\cdot\text{H}_2\text{O}$ is inhibited and therefore, liberation of hydrogen is stopped,^[57] thus showing no conversion of styrene. To support these findings, two addition control experiments were performed with homogeneous salts with identical Cu loadings present in Cu@ZIF-8 . The observed catalytic data indicated that 80 and 67% conversions of styrene are achieved with $\text{Cu}(\text{NO}_3)_2\cdot 3\text{H}_2\text{O}$ and CuI salts, respectively under similar conditions. Additionally, the physical mixture of the metal precursors of Cu@ZIF-8 was also examined in the

hydrogenation of styrene and observing 89% conversion under similar conditions. These control experiments unambiguously prove that the incorporated metal ions within the framework of ZIF-8 must be readily available to coordinate with $\text{N}_2\text{H}_4\cdot\text{H}_2\text{O}$. Thus, Cu^{2+} ion plays a crucial role in achieving quantitative conversion of styrene under these conditions. Furthermore, the homogeneous $\text{Cu}(\text{NO}_3)_2\cdot 3\text{H}_2\text{O}$ and CuI salts were deactivated after 7 h while Cu@ZIF-8 solid shows complete conversion of styrene without deactivation (Figure 10).

Table 1. Optimization of the reaction conditions for the hydrogenation of styrene.^a



Entry	Catalyst	Solvent	Reducing agent	Conversion ^b (%)
1	-	Ethanol	$\text{N}_2\text{H}_4\cdot\text{H}_2\text{O}$	20
2	ZIF-8	Ethanol	$\text{N}_2\text{H}_4\cdot\text{H}_2\text{O}$	36
3	Cu@ZIF-8	Ethanol	$\text{N}_2\text{H}_4\cdot\text{H}_2\text{O}$	>99
4	Cu@ZIF-8	Methanol	$\text{N}_2\text{H}_4\cdot\text{H}_2\text{O}$	80
5	Cu@ZIF-8	DCM	$\text{N}_2\text{H}_4\cdot\text{H}_2\text{O}$	38
6	Cu@ZIF-8	ACN	$\text{N}_2\text{H}_4\cdot\text{H}_2\text{O}$	47
7	Cu@ZIF-8	Toluene	$\text{N}_2\text{H}_4\cdot\text{H}_2\text{O}$	27
8	Cu@ZIF-8	Neat	$\text{N}_2\text{H}_4\cdot\text{H}_2\text{O}$	51
9	Cu@ZIF-8	Ethanol	Isopropanol	0
10 ^c	Cu@ZIF-8	Ethanol	$\text{N}_2\text{H}_4\cdot\text{H}_2\text{O}$	34
11 ^d	Cu@ZIF-8	Ethanol	$\text{N}_2\text{H}_4\cdot\text{H}_2\text{O}$	51
12 ^e	Cu@ZIF-8	Ethanol	$\text{N}_2\text{H}_4\cdot\text{H}_2\text{O}$	79
13 ^f	Cu@ZIF-8	Ethanol	$\text{N}_2\text{H}_4\cdot\text{H}_2\text{O}$	42
14 ^g	Cu@ZIF-8	Ethanol	$\text{N}_2\text{H}_4\cdot\text{H}_2\text{O}$	77
15 ^h	Cu@ZIF-8	Ethanol	$\text{N}_2\text{H}_4\cdot\text{H}_2\text{O}$	95
16 ⁱ	Cu@ZIF-8	Ethanol	$\text{N}_2\text{H}_4\cdot\text{H}_2\text{O}$	-
17	$\text{Cu}(\text{NO}_3)_2\cdot 3\text{H}_2\text{O}$	Ethanol	$\text{N}_2\text{H}_4\cdot\text{H}_2\text{O}$	80
18	CuI	Ethanol	$\text{N}_2\text{H}_4\cdot\text{H}_2\text{O}$	67
19	$\text{Cu}(\text{NO}_3)_2\cdot 3\text{H}_2\text{O} + \text{Zn}(\text{NO}_3)_2$	Ethanol	$\text{N}_2\text{H}_4\cdot\text{H}_2\text{O}$	89

^aReactions conditions: styrene (1 mmol), $\text{N}_2\text{H}_4\cdot\text{H}_2\text{O}$ (3 mmol), catalyst (20 mg), room temperature, 14 h.

^bDetermined by GC. Selectivity of ethylbenzene was always more than 99%.

^c Cu@ZIF-8 (5 mg)

^d Cu@ZIF-8 (10 mg)

^e Cu@ZIF-8 (15 mg)

^f $\text{N}_2\text{H}_4\cdot\text{H}_2\text{O}$ (1 mmol)

^g $\text{N}_2\text{H}_4\cdot\text{H}_2\text{O}$ (2 mmol)

^h after 3rd reuse

ⁱ pyridine (1 mmol).

The stability of Cu@ZIF-8 was assessed under the optimized reaction conditions by hot filtration and reusability tests. The styrene hydrogenation was performed with Cu@ZIF-8 solid and it was removed from the reaction mixture at around 30% conversion. The kinetics of the reaction was progressed in the absence of solid. Comparison of styrene conversion with and without solid catalysts revealed that the conversion rate is significantly affected upon removal of the solid. Hence, this experiment clearly rules out the contribution of the leached Cu^{2+} ions under these conditions, thus proving the heterogeneity of the process. Furthermore, reusability of Cu@ZIF-8 was also performed under the optimized reaction conditions. The catalytic results have shown that the activity of Cu@ZIF-8 is retained for three reuses with no significant decay in styrene conversion. ICP analysis of the three times reused solid showed 2.12 ppm of Cu, which is in agreement with the leaching and reusability results. In addition, powder XRD of the fresh and three times reused solids was compared and no significant changes are observed in the crystallinity as well as structural integrity of the reused solid compared to the fresh material (Figure S22). Further, morphology of the three times reused solid exhibited identical features to the fresh material (Figure 4). These catalytic data in combination with analytical and microscopic results clearly prove the robust nature of Cu@ZIF-8 under these conditions.

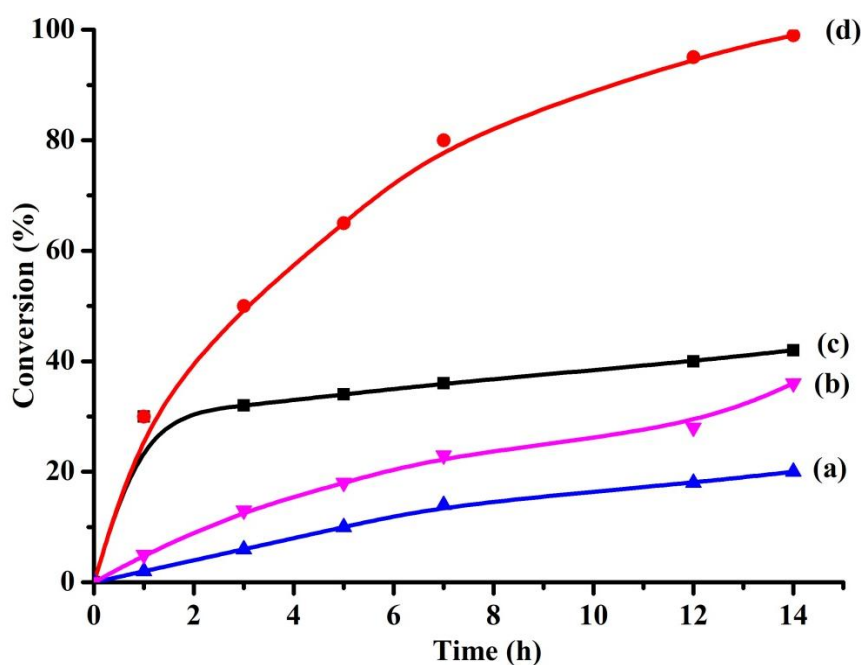


Figure 7. Time conversion plot for the hydrogenation of styrene to ethylbenzene (a) blank control without catalyst, (b) ZIF-8, (c) filtration of solid after 1 h and the reaction mixture stirred under identical reaction conditions and (d) Cu@ZIF-8.

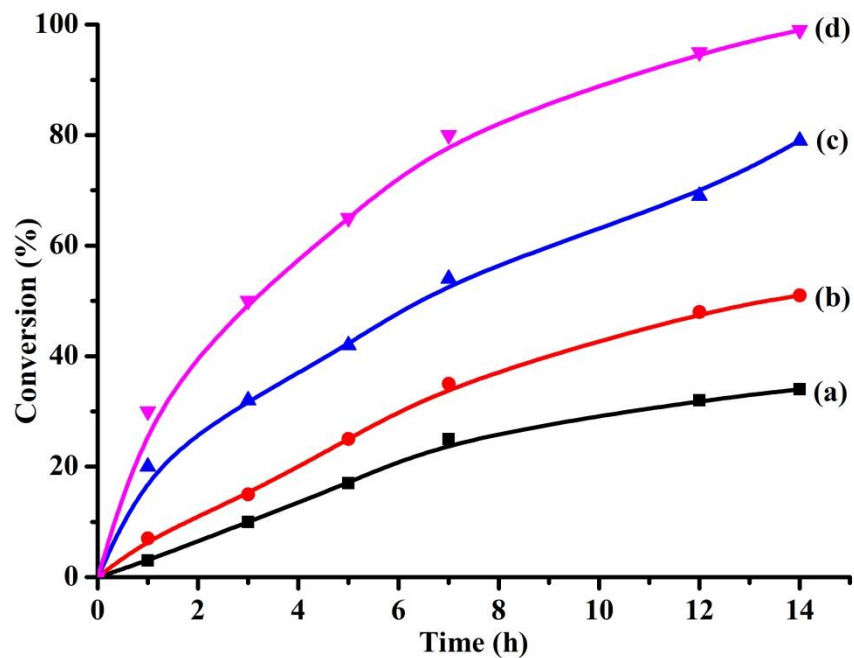


Figure 8. Hydrogenation of styrene using (a) 5 mg, (b) 10 mg, (c) 15 mg and (d) 20 mg Cu@ZIF-8 loadings..

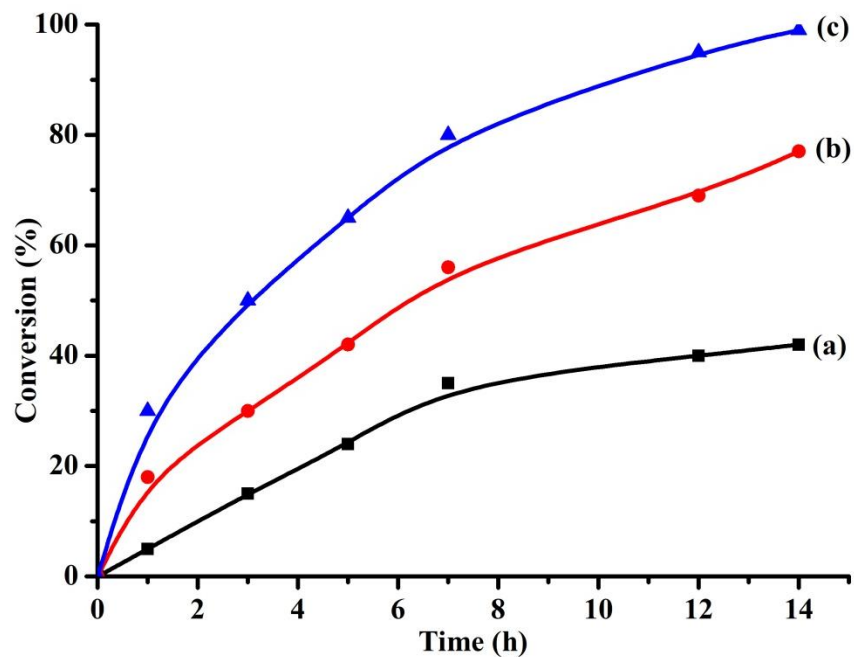


Figure 9. Hydrogenation of styrene using $\text{N}_2\text{H}_4 \cdot \text{H}_2\text{O}$ with (a) 1 mmol, (b) 2 mmol and (c) 3 mmol.

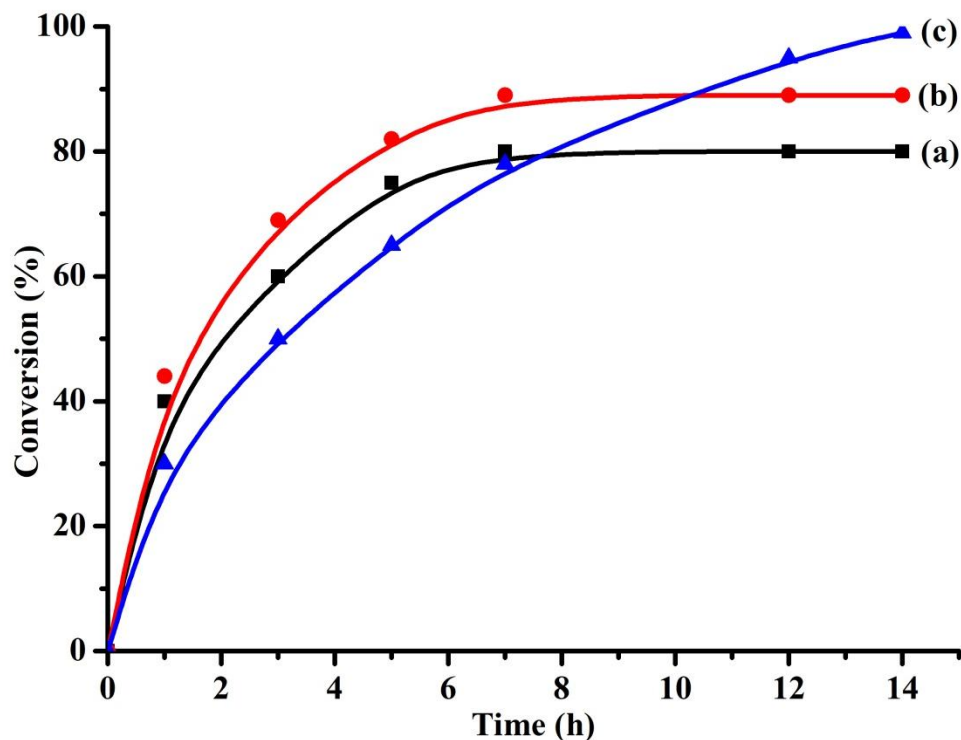
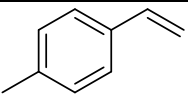
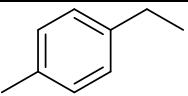
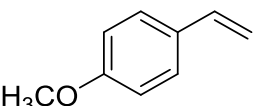
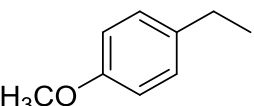
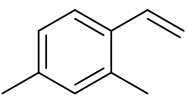
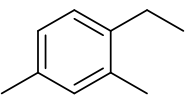
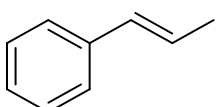
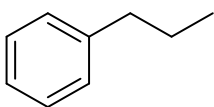
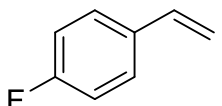
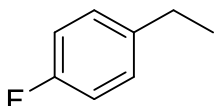
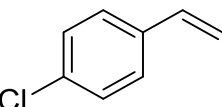
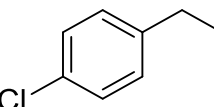
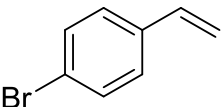
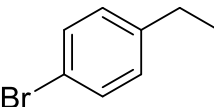
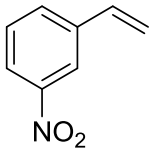
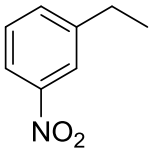
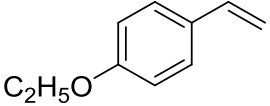
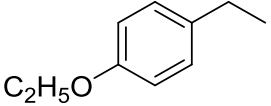
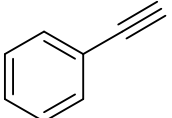
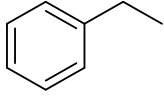


Figure 10. Hydrogenation of styrene using (a) $\text{Cu}(\text{NO}_3)_2 \cdot 3\text{H}_2\text{O}$, (b) $\text{Cu}(\text{NO}_3)_2 + \text{Zn}(\text{NO}_3)_2$ and (c) Cu@ZIF-8 .

With the optimized reaction conditions in hand, the promising activity and stability of Cu@ZIF-8 in the hydrogenation of styrene under mild reaction conditions prompted us to screen for other substituted styrene derivatives with electron donating and withdrawing substituents. The observed results are shown in Table 2. 4-Methyl and 4-methoxystyrenes afforded 100 and 97% conversions using Cu@ZIF-8 as catalyst in ethanol after 14 h. On the other hand, 2,4-dimethylstyrene was also converted to its respective product in 97% conversion under same conditions. The conversion of β -methylstyrene was decreased to 74% under identical conditions. This decrease in the conversion may be due to the diffusion limitation imposed by this branched olefin. 4-Fluoro, 4-chloro and 4-bromostyrenes were also quantitatively converted to their respective hydrogenated products. A significant decrease in the conversion was noticed for 3-nitrostyrene and is believed due to diffusion limitations. On other hand, 4-ethoxystyrene was also converted quantitatively to its corresponding hydrogenated product. Finally, phenylacetylene was hydrogenated at 61% conversion with the selectivity of ethylbenzene to 78% while styrene selectivity to 22%.

Table 2. Hydrogenation of various alkenes using Cu@ZIF-8 as a solid catalyst.^a

Entry	Conversion (%) ^b	Substrate	Product
1	100		
2	97		
3	97		
4	74		
5	99		
6	100		
7	99		
8	20		
9	99		
10 ^c	61		

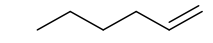
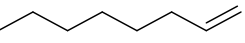
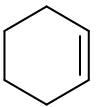
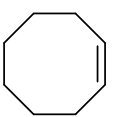
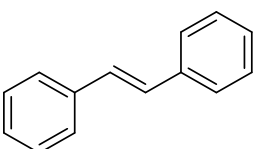
^aReaction conditions: Substrate (1 mmol), N₂H₄·H₂O (3 mmol), Cu@ZIF-8 (20 mg), ethanol (1 mL), room temperature, 14 h.

^bConversion of substrate was determined by GC using internal standard method. The selectivity of the reduced products was always more than 99 %.

^cSelectivity of ethylbenzene was 78 % while styrene was 22 %.

After demonstrating the stability and wide substrate scope of Cu@ZIF-8, size selective hydrogenation of olefins within the constrained spaces of ZIF-8 was performed and the observed catalytic data are discussed. For this study, 1-hexene, 1-octene, cyclohexene, cyclooctene and t-stilbene were selected as model olefins with varying molecular dimensions (Table 3). Hydrogenation of 1-hexene to 1-hexane was selectively achieved with Cu@ZIF-8 at 92% conversion due to its smaller dimension than the pore aperture of Cu@ZIF-8 (3.4 Å). Similarly, 1-octene and cyclohexene exhibited 84 and 80% conversions to their respective hydrogenated products, respectively. This slightly lower conversion of these substrates is due to their larger dimensions than to 1-hexene. The conversion of cyclooctene was further decreased due to its bigger size than the pore size of Cu@ZIF-8. Importantly, the conversion of t-stilbene was significantly decreased to 12% due to its larger size than the rest of the olefins. These catalytic data convincingly prove that the conversion of olefins is gradually decreased upon increasing molecular dimension of olefins. Hence, these experimental data prove that the hydrogenation reaction occurs within the confinement of Cu@ZIF-8 pores.

Table 3. Size selective hydrogenation of various alkenes between Cu@ZIF-8 and Cu/ZIF-8 as solid catalysts.^a

Entry	Substrate	Molecular dimension (Å)	Conversion (%)			
			Cu@ZIF-8		Cu/ZIF-8	
			1 h	14 h	1 h	14 h
1		2.5	20	84	38	99
2		4	24	92	48	99
3		4.2	15	80	40	96
4		5.5	14	71	61	100
5		5.6	2	12	16	36

^aReaction conditions: Substrate (1 mmol), N₂H₄·H₂O (3 mmol), catalyst (20 mg), ethanol (1 mL), RT, 14 h.

^bDetermined by GC.

Figure 11 provides the conversion of 1-hexene, 1-octene, cyclohexene, cyclooctene and t-stilbene using Cu@ZIF-8 and Cu/ZIF-8 after 1 h (Figure S6 after 14 h) under the optimized reaction

conditions. These catalytic data suggest that the initial reaction rate is relatively much higher for all these olefins irrespective of their molecular dimensions with Cu/ZIF-8 compared to Cu@ZIF-8 (Figures S1-S5). This enhanced activity of Cu/ZIF-8 than to Cu@ZIF-8 is that Cu^{2+} ions are adsorbed on the exterior surface of ZIF-8 that can be readily accessed by the reactants without diffusion limitations (Figure S26). In contrast, the reaction rate was highly controlled by molecular dimensions of olefins using Cu@ZIF-8 as catalyst and is due to the diffusion limitations encountered by larger size of olefin to access Cu^{2+} ions within the framework. These notable differences in the activity between Cu@ZIF-8 and Cu/ZIF-8 clearly indicate the operation of size selective hydrogenation with Cu@ZIF-8 as heterogeneous catalyst under these conditions.

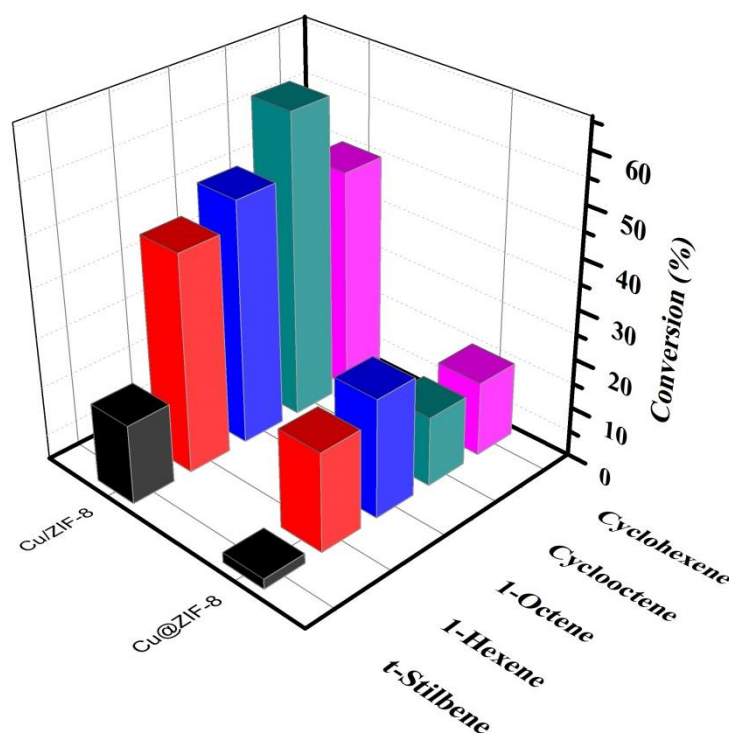


Figure 11. Size selective hydrogenation of various alkenes using Cu@ZIF-8 versus Cu/ZIF-8 after 1 h.

Table S1 provides the comparison of the hydrogenation of styrene with Cu@ZIF-8 with other reported solid catalysts in the literature. These results clearly indicate that most of the hydrogenation reactions have been performed with noble metal NPs as the active sites. Some of the catalytic systems have also been reported at elevated temperature (60 or 101 °C). On the other hand, the hydrogenation of styrene to ethylbenzene using $\text{Cu}_3(\text{BTC})_2$ with hydrazine hydrate resulted in 60% conversion after 24 h.

Interestingly, the present catalytic system with relatively lower Cu^{2+} loading in Cu@ZIF-8 in respect to $\text{Cu}_3(\text{BTC})_2$ afforded much superior activity at shorter reaction time. Furthermore, Table S2 shows the list of catalysts that have been reported for the size selective MOF catalysts for the hydrogenation of olefins. These results clearly indicate that no attempts were made to use framework cations as active sites for the hydrogenation of olefins. Hence, this is the first report showing the catalytic performance of mixed-metal MOFs, Cu@ZIF-8 as a size selective heterogeneous catalyst for the hydrogenation of olefins.

3. Conclusions

In summary, Cu@ZIF-8 and Cu/ZIF-8 solids were synthesized and the former solid is characterized by suitable spectroscopic, microscopic techniques. Besides showing the activity of Cu@ZIF-8 for the hydrogenation of styrene and its derivatives at higher conversions to their corresponding saturated benzylic hydrocarbons with high selectivities, the size selective hydrogenation of Cu@ZIF-8 is clearly proved by comparing its activity with Cu/ZIF-8 under similar experimental conditions. Cu/ZIF-8 showed no discrimination among the various olefins tested but, in contrast Cu@ZIF-8 showed hydrogenation activity to those olefins having lower dimensions than the pore aperture of ZIF-8. These catalytic data convincingly demonstrate the occurrence of size selective hydrogenation of olefins with Cu@ZIF-8 . This work clearly illustrates the catalytic performance of the framework metal ions acting as active sites to promote hydrogenation of olefins compared to other reports involving metal NPs embedded on MOFs.

4. Experimental procedure

4.1 Materials

$\text{Cu}(\text{NO}_3)_2 \cdot 3\text{H}_2\text{O}$, $\text{Zn}(\text{NO}_3)_2 \cdot 6\text{H}_2\text{O}$, 2-methylimidazole, styrene and other alkenes derivatives were purchased from Sigma Aldrich and used as received. Solvents were also received from Sigma Aldrich and used as received without any further purification.

4.2 Instrumentation

Powder XRD diffraction patterns were recorded with Philips X'Pert diffractometer in the reflection mode having $\text{CuK}\alpha$ radiation ($\lambda = 1.5417 \text{ \AA}$) as the incident beam, PW3050/60 (2 theta) as Goniometer. UV-Visible DRS spectra were measured by Shimadzu UV-2700; ISR-2600 plus instrument in the range

between 200-800 nm by dispersing the sample on BaSO₄ surface. FT-IR spectra were measured in the range of 400-4000 cm⁻¹ using Bruker tensor 27 series FT-IR spectrometer. SEM images were measured with Hitachi S-3000H scanning electron microscope. Gas chromatography (GC) Agilent 7820A model was used for the determination of conversion and selectivity using high pure nitrogen as carrier gas with flame ionization detector. GC coupled with mass spectrometry (GC-MS) was employed under identical conditions for the confirmation of the products.

4.3 Synthesis of Cu@ZIF-8

Cu@ZIF-8 was prepared by following the procedure of Schneider and coworkers^[49] with a slight modification. Briefly, Cu(NO₃)₂·3H₂O and Zn(NO₃)₂·6H₂O (total 2 mmol) were dissolved in 22.6 mL methanol and 2-methylimidazole (1320 mg, 16 mmol) was dissolved in 22.6 mL of methanol separately. Then, these two solutions were mixed in drop wise by adding 2-methylimidazole solution to Zn²⁺ and Cu²⁺ solutions in a two-neck flask. The synthesis was conducted at room temperature under nitrogen flow with stirring for 1 h and later, it was kept for 24 h at room temperature. Cu@ZIF-8 solids were separated through centrifugation, followed by washing with methanol (3x 30 mL). The isolated Cu@ZIF-8 solid was dried in air oven at 60 °C for 6 h before analysis. The vials containing Cu@ ZIF-8 powders were tightly capped and stored at room temperature for further catalytic experiments.

4.4 Synthesis of Cu/ZIF-8

A metal solution was prepared by dissolving Cu(NO₃)₂·3H₂O (10 mg) in 22.6 mL methanol which is identical to the Cu loading in Cu@ZIF-8. Then, in a two-neck flask, ZIF-8 (100 mg) was added to Cu(NO₃)₂·3H₂O solution under nitrogen flow at room temperature with stirring for 1h. Later, Cu/ZIF-8 solids were separated by centrifugation and washed with methanol (2x 30 mL). The material was dried in air oven at 60°C for 6 h before catalytic experiments.

4.5 Experimental procedure

In a typical hydrogenation reaction, 20 mg of Cu@ZIF-8 was added to the high pressure tube containing styrene (1 mmol), hydrazine hydrate (3 mmol) and ethanol (1 mL). This reaction tube was sealed by silicon rubber septum and this reaction mixture was stirred at room temperature for the required time as shown in tables. The reaction progress was monitored by GC and after completion of the reaction, the mixture was washed three times with acetonitrile and filtered. Then, the product was

analyzed by GC to determine final conversion and selectivity. Conversion of olefin was determined by Agilent 7820 A using internal standard method and the formed products were confirmed by GC-MS (Figures S7-S21). The above described procedure was repeated for reusability tests with the recovered solid catalyst. Control experiments were performed with $\text{Cu}(\text{NO}_3)_2 \cdot 3\text{H}_2\text{O}$ (15 mg) and CuI (9 mg) as homogeneous catalysts under identical conditions with similar copper loadings as in the case of Cu@ZIF-8 . The physical mixture of $\text{Cu}(\text{NO}_3)_2 \cdot 3\text{H}_2\text{O}$ (15 mg) and $\text{Zn}(\text{NO}_3)_2 \cdot 6\text{H}_2\text{O}$ (148 mg) was used under similar conditions for the hydrogenation reaction.

Acknowledgements

A.D. extends his thanks to University Grants Commission (UGC), New Delhi, for awarding Assistant Professorship through Faculty Recharge Programme.

Conflict of Interest

The authors declare no conflict of interest.

Keywords: Hydrogenation of olefins · Heterogeneous catalysis · Metal-organic frameworks · Porous solids · Size selectivity

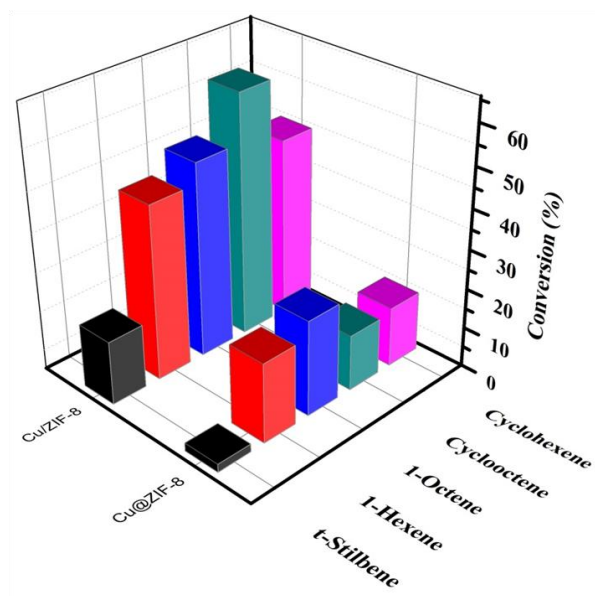
References

- [1] H. Li, M. Eddaoudi, M. O'Keeffe, O. M. Yaghi, *Nature* **1999**, *402*, 276-279.
- [2] H. Furukawa, K. E. Cordova, M. O'Keeffe, O. M. Yaghi, *Science* **2013**, *341*, 1230444.
- [3] S. L. James, *Chem. Soc. Rev.* **2003** *32*, 276-288.
- [4] A. Corma, H. García, F. X. Llabrés I Xamena, *Chem. Rev.* **2010** *110*, 4606-4655.
- [5] S. Kitagawa, R. Kitaura, S.-I. Noro, *Angew. Chem. Int. Ed.* **2004** *43*, 2334-2375.
- [6] J. L. C. Rowsell, O. M. Yaghi, *Micropor. Mesopor. Mater.* **2004** *73*, 3-14.
- [7] S. T. Meek, J. A. Greathouse, M. D. Allendorf, *Adv. Mater.* **2011**, *23*, 249-267.
- [8] S. Qiu, G. Zhu, *Coord. Chem. Rev.* **2009**, *253*, 2891-2911.
- [9] K. Koh, A. G. Wong-Foy, A. J. Matzger, *Angew. Chem. Int. Ed.* **2008**, *47*, 677-680.
- [10] A. Dhakshinamoorthy, H. Garcia, *Chem. Soc. Rev.* **2012**, *41*, 5262-5284.
- [11] Q. Yang, Q. Xu, H.-L. Jiang, *Chem. Soc. Rev.* **2017**, *46*, 4774-4808.
- [12] H. R. Moon, D.-W. Lim, M. P. Suh, *Chem. Soc. Rev.* **2013**, *42*, 1807-1824.
- [13] X. Fang, Q. Shang, Y. Wang, L. Jiao, T. Yao, Y. Li, Q. Zhang, Y. Luo, H.-L. Jiang, *Adv. Mater.* **2018**, *30*, 1705112.
- [14] C.-C. Wang, X.-D. Du, J. Li, X.-X. Guo, P. Wang, J. Zhang, *Appl. Catal. B: Environ.* **2016**, *193*, 198-216.
- [15] H.-U. Blaser, C. Malan, B. Pugin, F. Spindler, H. Steiner, M. Studer, *Adv. Synth. Catal.* **2003** *345*, 103-151.
- [16] J. J. Verendel, O. Pàmies, M. Diéguez, P. G. Andersson, *Chem. Rev.* **2014**, *114*, 2130-2169.

- [17] X.-F. Yang, A. Wang, B. Qiao, J. Li, J. Liu, T. Zhang, *Acc. Chem. Res.* **2013**, *46*, 1740-1748.
- [18] A. B. Laursen, K. T. Højholt, L. F. Lundegaard, S. B. Simonsen, S. Helveg, F. Schüth, M. Paul, J.-D. Grunwaldt, S. Kegnoes, C. H. Christensen, K. Egeblad, *Angew. Chem. Int. Ed.* **2010**, *49*, 3504-3507.
- [19] C. Liu, J. Liu, S. Yang, C. Cao, W. Song, *ChemCatChem* **2016**, *8*, 1279-1282.
- [20] F. Wang, J. Ren, Y. Cai, L. Sun, C. Chen, S. Liang, X. Jiang, *Chem. Eng. J.* **2016**, *283*, 922-928.
- [21] A. R. Morgado Prates, F. Meunier, M. Dodin, R. Martinez Franco, D. Farrusseng, A. Tuel, *Chem. Eur. J.* **2019**, *25*, 2972-2977.
- [22] A. Zanon, F. Verpoort, *Coord. Chem. Rev.* **2017**, *353*, 201-222.
- [23] A. Dhakshinamoorthy, A. M. Asiri, H. Garcia, *ChemCatChem* **2020**, *12*, 4732-4753.
- [24] Q. Yang, Q. Xu, S.-H. Yu, H.-L. Jiang, *Angew. Chem. Int. Ed.* **2016**, *55*, 3685-3689.
- [25] Y. Yang, F. Wang, Q. Yang, Y. Hu, H. Yan, Y.-Z. Chen, H. Liu, G. Zhang, J. Lu, H.-L. Jiang, H. Xu, *ACS Appl. Mater. Interfaces* **2014**, *6*, 18163-18171.
- [26] X. Wang, M. Li, C. Cao, C. Liu, J. Liu, Y. Zhu, S. Zhang, W. Song, *ChemCatChem* **2016**, *8*, 3224-3228.
- [27] P. Wang, J. Zhao, X. Li, Y. Yang, Q. Yang, C. Li, *Chem. Commun.* **2013**, *49*, 3330-3332.
- [28] B. Wang, W. Liu, W. Zhang, J. Liu, *Nano Res.* **2017**, *10*, 3826-3835.
- [29] W. Zhang, G. Lu, C. Cui, Y. Liu, S. Li, W. Yan, C. Xing, Y. R. Chi, Y. Yang, F. Huo, *Adv. Mater.* **2014**, *26*, 4056-4060.
- [30] S. Aguado, S. El-Jamal, F. Meunier, J. Canivet, D. Farrusseng, *Chem. Commun.* **2016**, *52*, 7161-7163.
- [31] Y. Jiang, X. Zhang, X. Dai, Q. Sheng, H. Zhuo, J. Yong, Y. Wang, K. Yu, L. Yu, C. Luan, H. Wang, Y. Zhu, X. Duan, P. Che, *Chem. Mater.* **2017**, *29*, 6336-6345.
- [32] L.-N. Chen, H.-Q. Li, M.-W. Yan, C.-F. Yuan, W.-W. Zhan, Y.-Q. Jiang, Z.-X. Xie, Q. Kuang, L.-S. Zheng, *Small* **2017**, *13*, 1700683.
- [33] P. Koley, S. C. Shit, B. Joseph, S. Pollastri, Y. M. Sabri, E. L. H. Mayes, L. Nakka, J. Tardio, J. Mondal, *ACS Appl. Mater. Interfaces* **2020**, *12*, 21682-21700.
- [34] C. Sarkar, R. Paul, S. C. Shit, Q. T. Trinh, P. Koley, B. S. Rao, A. M. Beale, C.-W. Pao, A. Banerjee, J. Mondal, *ACS Sustain. Chem. Eng.* **2021**, *9*, 2136-2151.
- [35] X. C. Huang, Y. Y. Lin, J. P. Zhang, X. M. Chen, *Angew. Chem., Int. Ed.* **2006**, *45*, 1557-1559.
- [36] B. Wang, A. P. Côté, H. Furukawa, M. O'Keeffe, O. M. Yaghi, *Nature* **2008**, *453*, 207-211.
- [37] B. A. Al-Maythaly, O. Shekhah, R. Swaidan, Y. Belmabkhout, I. Pinnau, M. Eddaoudi, *J. Am. Chem. Soc.* **2015**, *137*, 1754-1757.
- [38] L. J. Murray, M. Dinca, J. R. Long, *Chem. Soc. Rev.* **2009**, *38*, 1294-1314.
- [39] H. Liu, L. Chang, L. Chen, Y. Li, *J. Mater. Chem. A* **2015**, *3*, 8028-8033.
- [40] L. E. Kreno, K. Leong, O. K. Farha, M. Allendorf, R. P. Van Duyne, J. T. Hupp, *Chem. Rev.* **2012**, *112*, 1105-1125.
- [41] J. R. Li, J. Sculley, H.-C. Zhou, *Chem. Rev.* **2012**, *112*, 869-932.
- [42] J. Zhuang, C. H. Kuo, L. Y. Chou, D. Y. Liu, E. Weerapana, C. K. Tsung, *ACS Nano* **2014**, *8*, 2812-2819.
- [43] B. Chen, Z. Yang, Y. Zhu, Y. Xia, *J. Mater. Chem. A* **2014**, *2*, 16811-16831.
- [44] S. R. Venna, J. B. Jasinski, M. A. Carreon, *J. Am. Chem. Soc.* **2010**, *132*, 18030.
- [45] L. H. Wee, Y. Li, K. Zhang, P. Davit, S. Bordiga, J. Jiang, I. F. J. Vankelecom, J. A. Martens, *Adv. Funct. Mater.* **2015**, *25*, 516.
- [46] A. Bétard, R. A. Fischer, *Chem. Rev.* **2012**, *112*, 1055-1083.
- [47] A. Dhakshinamoorthy, A. M. Asiri, H. Garcia, *Catal. Sci. Technol.* **2016**, *6*, 5238-5261.
- [48] M. Y. Masoomi, A. Morsali, A. Dhakshinamoorthy, H. Garcia, *Angew. Chem. Int. Ed.* **2019**, *58*, 15188-15205.
- [49] A. Schejn, A. Aboulaich, L. Balan, V. Falk, J. Lalevée, G. Medjahdi, L. Aranda, K. Mozeta, R. Schneider, *Catal. Sci. Technol.* **2015**, *5*, 1829-1839.

- [50] N. Nagarjun, A. Dhakshinamoorthy, *New J. Chem.* **2019**, *43*, 18702-18712.
- [51] R. Li, X. Ren, H. Ma, X. Feng, Z. Lin, X. Li, C. Hu, B. Wang, *J. Mater. Chem. A* **2014**, *2*, 5724-5727.
- [52] R. Li, X. Ren, X. Feng, X. Li, C. Hu, B. Wang, *Chem. Commun.* **2014**, *50*, 6894-6897.
- [53] Y. Du, R. Z. Chen, J. F. Yao, H. T. Wang, *J. Alloys Compd.* **2013**, *551*, 125-130.
- [54] S. Goyal, M. S. Shaharun, C. F. Kait, B. Abdulla, *J. Phys. Conf. Ser.* **2018**, *1123*, 012062.
- [55] R. Dang, Q. Li, M. Chen, Z. Hu, X. Xiao, *Phys.Chem.Chem.Phys.* **2019**, *21*, 314-321.
- [56] J. Gu, Y. Xie, W. Chen, C. Hu, F. Qiao, Z. Xu, X. Liu, X. Zhao, G. Zhang, *CrystEngComm* **2018**, *20*, 6565-6572
- [57] P. Garcia-Garcia, M. Muller, A. Corma, *Chem. Sci.* **2014**, *5*, 2979-3007.

Table of Contents



Cu²⁺-doped ZIF-8 (Cu@ZIF-8) is reported as a reusable heterogeneous solid catalyst for the hydrogenation of styrenes to their respective reduced products using hydrazine hydrate as a reducing agent at room temperature. Further, Cu@ZIF-8 is also shown to exhibit size selective catalysis, thus proving the occurrence of reduction within the pores of Cu@ZIF-8.